Supporting Information

Asymmetric copper and boron dual-sites synergy for boosting conversion of carbon monoxide into C_2 products under visible light

Tianwei He[1], Karsten Reuter[2] and Aijun Du[1,]*

[1]School of Chemistry, Physics and Mechanical Engineering, Queensland University of Technology, Garden Point Campus, QLD 4001, Brisbane, Australia

[2]Chair for Theoretical Chemistry and Catalysis Research Center, Technical University of Munich, Lichtenbergstrasse 4, Garching 85747, Germany

The formation energy of an atom or atom pair on g-C_3N_4 is calculated as:

$$E_{binding} = E_{M@g-C3N4} - E_M - E_{g-C3N4},$$

where $E_{M@g-C3N4}$, E_M and E_{g-C3N4} are the total energy of the single atom or atom pair anchored on the g-C_3N_4 sheet, of the single atom or atom pair, and of g-C_3N_4, respectively.

The Gibbs free energy for each state was calculated based on the computational hydrogen electrode model proposed by Nørskov et al[1, 2], which can be described by:

$$G = E + ZPE + \int C_p dT - TS$$

Where zero point energies (ZPE), enthalpic temperature correction ($\int C_p dT$) and entropy correction (TS) were obtained from the vibrational frequency calculations at 298.15 K and presented in Table S1. Gas-phase free energies were obtained by standard methods[3] (Table S1). The vibration analysis for intermediate states, frequencies were calculated by treating all 3N degrees using the following equations:

$$E_{ZPE} = \frac{1}{2}\sum_i h\nu_i$$

$$-TS = K_B T \sum_i \ln\left(1 - e^{-\frac{hv_i}{K_B T}}\right) - \sum_i hv_i \left(\frac{1}{e^{\frac{hv_i}{K_B T}} - 1}\right)$$

where h, v, K_B are the Planck constant, vibrational frequencies and Boltzman constant, respectively.

The adsorption energy of a CO molecule on the active sites was calculated by equation:

$$E_{ad} = E_{*CO} - E_{*} - E_{CO(gas)}$$

where E_{*CO} refers to the total energy for a CO molecule absorbed on the catalyst; E_{*} is the total energy of the bare catalyst and $E_{CO(gas)}$ is the carbon monoxide gas phase energy. Here, the more negative value of the adsorption energy stands for a stronger binding strength of the CO molecular.

The Gibbs free energy change (ΔG) between any two elemental steps were calculated by:

$$\Delta G = \Delta E + \Delta E_{ZPE} + \int C_p dT - T\Delta S + eU + \Delta G_{pH}$$

where ΔE is the electronic energy difference between the free standing and the adsorption states of the intermediates; ΔE_{ZPE} and ΔS are the changes of zero point energies and entropy. e and U are the number of electrons transferred and the electrode potential applied; ΔG_{pH} is the free energy correction of pH, which can be calculated by:

$$\Delta G_{pH} = k_B T \times pH \times ln10$$

The overpotential was defined by calculating the lowest positive elementary free energy change between any two steps. It is invariable and will not be influenced by the pH values. Therefore, the pH was set to zero in this work.

To calculate the free energies of the different intermediates in the catalytic process, we employed the computational hydrogen electrode (CHE) model to include the electrode potential correction to the free energy of each state, by considering the electrochemical proton-electron transfer being a function to the applied electrical potential[2, 4]. For this model, the free energy of a proton-electron pair at oV *vs* RHE is defined as ½ of the

H2 free energy at 101,325 Pa pressure. The free energy for each intermediate is then a function of the electrode potential (U) at 298.15 K according to the equation: $G(U) = G(0V) - neU$. Where e refers to the elementary charge of an electron, n represents the number of proton-electron pair transferred to the investigated intermediate or the final states. The application of the equation to an elementary reaction pathway results in the electrode potential corrected free energy pathway, therefore provides a venue to evaluate at which potential a certain CO electroreduction pathway opens, as well as defining the potential dependent reaction step. In the current study, the relative free energies of the reaction intermediates were taken only as an indication the starting point of different pathways in the electroreduction of CO2, since reaction barriers were not considered. As shown in previous studies, barriers for proton transfer to adsorbates from solution are normally low enough to be surmountable at room temperatures [1, 5, 6].

Table S1. Computed frequencies (in me V) and corresponding thermodynamic energy correction (in eV) for the different adsorbates and some gas phase, where the * refers to the active site.

Adsorption Species	**ZPE**	$\int C_p dT$	**TS**
*CO-*CO	0.414	0.138	0.306
*OCCO	0.429	0.118	0.243
*HOCCO	0.743	0.132	0.258
*HOCCOH	1.084	0.126	0.241
*OCC	0.368	0.059	0.122
*CCHO	0.636	0.09	0.186
*CHCO	0.643	0.084	0.158
*HOCHCOH	1.373	0.133	0.253
*HOCCH	0.959	0.087	0.156
*HOCHCH	1.282	0.094	0.170
*HOCHCHOH	1.654	0.094	0.248
*CH_2CH	1.162	0.056	0.09
*CHCH	0.804	0.061	0.102
*$HOCH_2CH$	1.567	0.111	0.221

*$HOCH_2CH_2$	1.862	0.128	0.264
*$HOCH_2CHOH$	1.981	0.158	0.333
*CH_2CH_2	1.436	0.068	0.116
*H	0.239	0.005	0.007
CO	0.122	0.096	0.618
C_2H_4	1.358	0.109	0.428
CH_3CH_2OH (g)	2.109	0.138	0.566

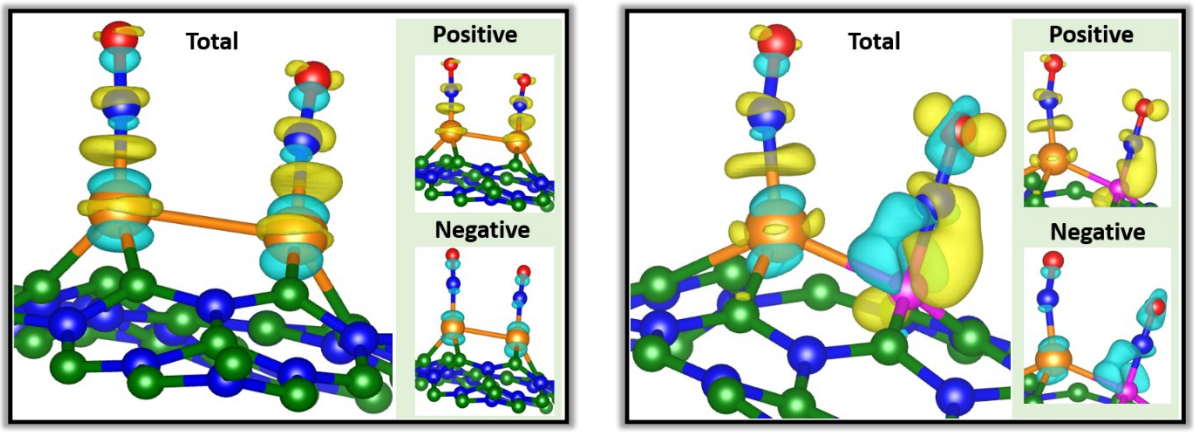

Figure S1 The charge difference density of Cu-Cu/g-C3N4 and Cu-B/g-C3N4 with the adsorption of two CO molecules, where the isosurface value is set to be 0.005 e/Å and the positive and negative charges are shown separately in yellow and cyan. Green, blue, bronze, pink, red and white balls represent the N, C, Cu B, O and H atoms, respectively.

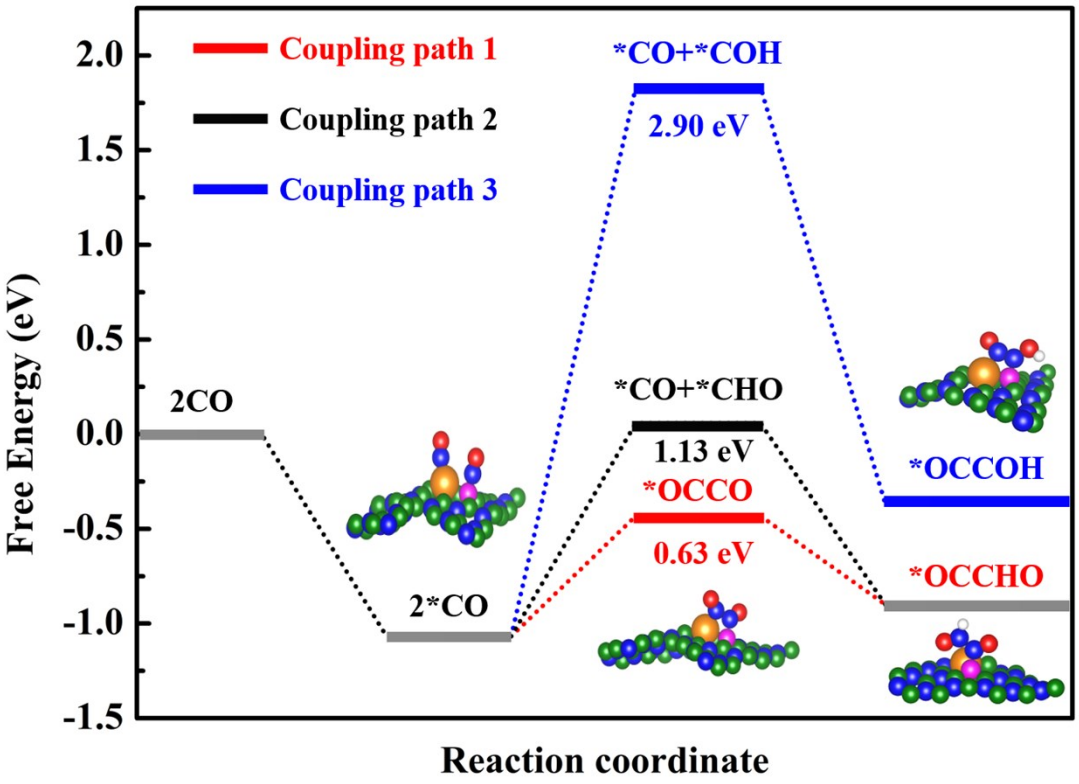

Figure S2 Calculated free energy profiles of different C-C coupling paths at open circuit voltage (o V vs. the reducible hydrogen electrode, RHE). Inserts show the corresponding structures of the reaction intermediates. Green, blue, bronze, pink, red and white balls represent N, C, Cu, B, O and H atoms, respectively.

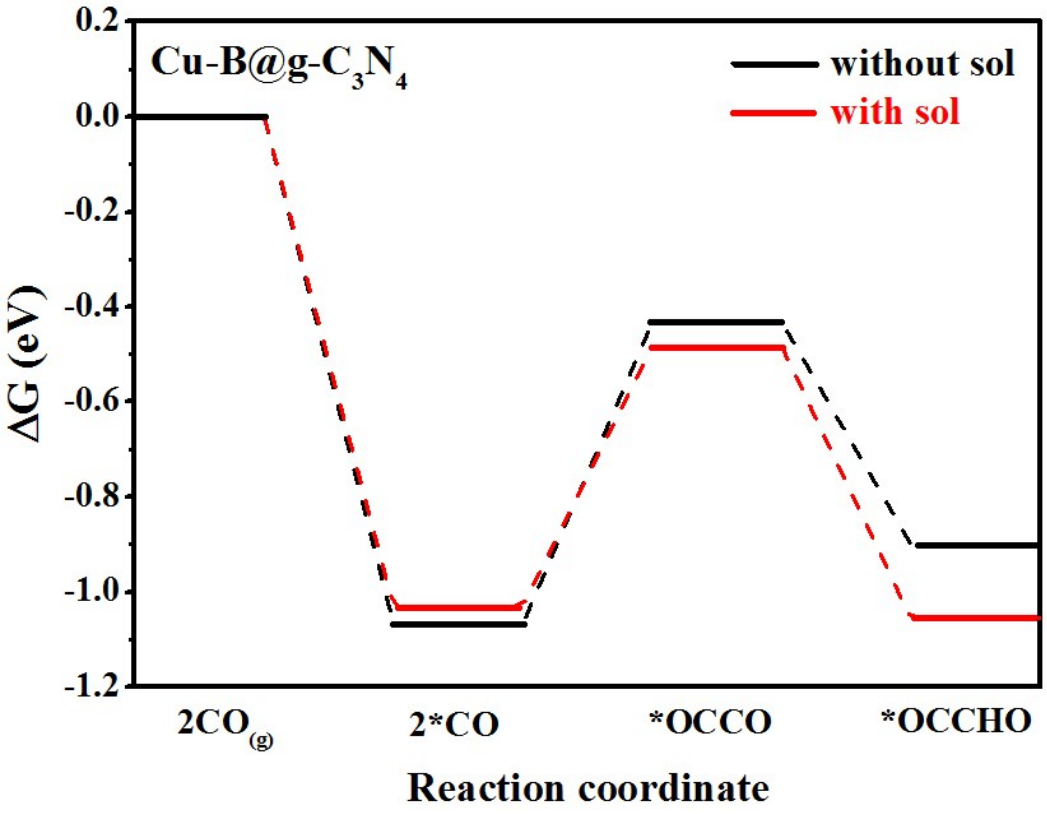

Figure S3 Evaluation of the influence of solvent effect on the Gibbs free energy change during the reaction process.

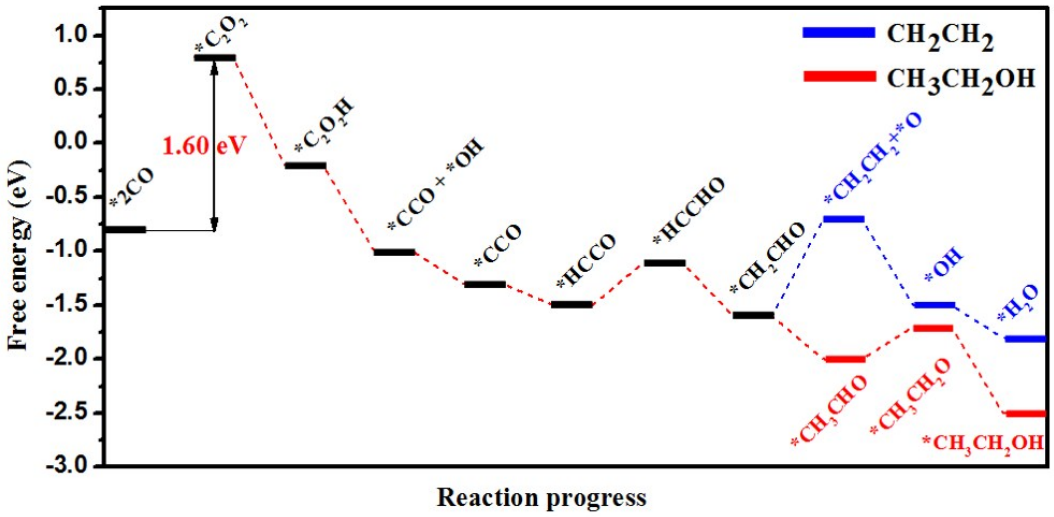

Figure S4 Redraw the free energy diagram of CO reduction to CH_2CH_2 and CH_3CH_2OH on B doped Cu (111) surface according to ref.3[7].

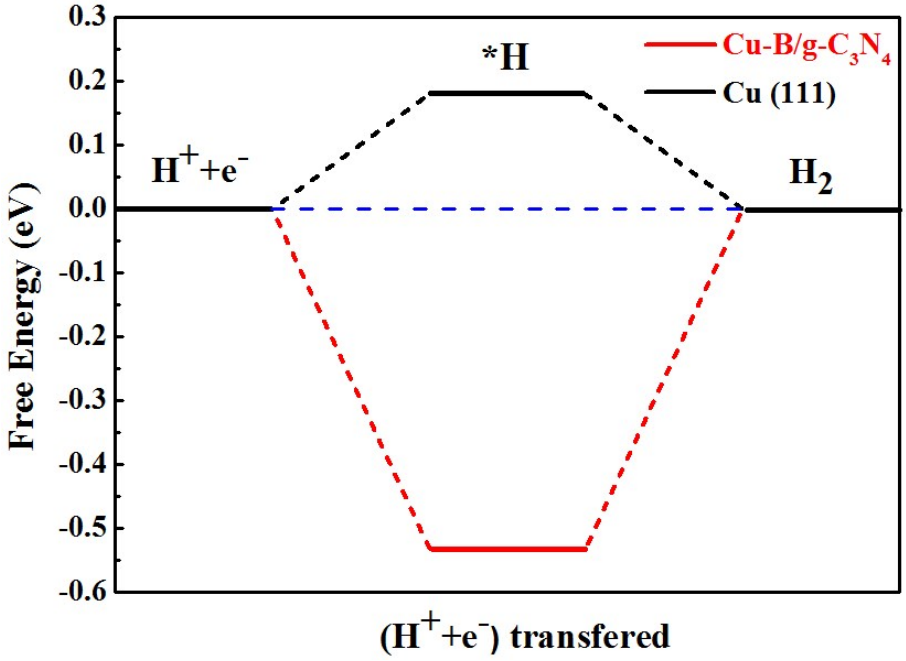

Figure S5 Comparison of the hydrogen evolution reaction activity on Cu-B/g-C_3N_4 and Cu (111) surface.

[1] Peterson, A. A.; Abild-Pedersen, F.; Studt, F.; Rossmeisl, J.; Nørskov, J. K. How copper catalyzes the electroreduction of carbon dioxide into hydrocarbon fuels. *Energy Environ. Sci.* **2010,** *3*, 1311-1315.

[2] Nørskov, J. K.; Rossmeisl, J.; Logadottir, A.; Lindqvist, L.; Kitchin, J. R.; Bligaard, T.; Jonsson, H. Origin of the overpotential for oxygen reduction at a fuel-cell cathode. *J. Phys. Chem. B* **2004,** *108*, 17886-17892.

[3] Cramer, C. J.; Bickelhaupt, F. Essentials of computational chemistry. *Angew. Chem. Int. Ed.* **2003,** *42*, 381-381.

[4] Jiao, Y.; Zheng, Y.; Jaroniec, M.; Qiao, S. Z. Origin of the electrocatalytic oxygen reduction activity of graphene-based catalysts: A roadmap to achieve the best performance. *J. Am. Chem. Soc.* **2014,** *136*, 4394-4403.

[5] Shi, C.; Chan, K.; Yoo, J. S.; Nørskov, J. K. Barriers of electrochemical co2 reduction on transition metals. *Org. Process. Res. Dev.* **2016,** *20*, 1424-1430.

[6] Jiao, Y.; Zheng, Y.; Chen, P.; Jaroniec, M.; Qiao, S.-Z. Molecular scaffolding strategy with synergistic active centers to facilitate electrocatalytic co2 reduction to hydrocarbon/alcohol. *J. Am. Chem. Soc.* **2017,** *139*, 18093-18100.

[7] Zhou, Y.; Che, F.; Liu, M.; Zou, C.; Liang, Z.; De Luna, P.; Yuan, H.; Li, J.; Wang, Z.; Xie, H. Dopant-induced electron localization drives co 2 reduction to c 2 hydrocarbons. *Nat. Chem.* **2018,** *10*, 974.